JOURNAL OF MATERIALS SCIENCE **35** (2000) 1205 – 1211

The porosity dependence of flexural modulus and strength for capsule-free hot isostatically pressed porous alumina

Y. B. P. KWAN
ASM Lithography B.V., De Run 1110, 5503 LA Veldhoven, Holland
D. J. STEPHENSON, J. R. ALCOCK
School of Industrial and Manufacturing Science, Cranfield University, Cranfield, MK43 0AL, UK
E-mail: j.r.alcock@cranfield.ac.uk

Structural properties such as flexural moduli and strength have been measured for a range of porous alumina specimens of different initial powder sizes and final porosities, sintered using the capsule-free hot isostatic pressing method. This processing method produces a porous body in which the closed porosity is negligible. The relationship of these structural properties to total porosity has been investigated. The results indicate that both a power and an exponential function could adequately describe the porosity dependence of flexural strength. The strength values obtained were test method dependent, and were significantly lower for specimens with sintering aids. A power law model based on a critical porosity, as proposed by Phani, gave the best fit for the modulus measurement data. No dependence of mechanical properties on particle size was observed. The strength measurement results did not appear to support suggestions that better strength could be obtained by the capsule-free hot isostatic pressing method than conventional sintering, as reported elsewhere.

1. Introduction

Porous ceramic materials are typically found in filtration applications where their high strength, high operating temperature and chemical inertness are of importance. Recently, there has been an increased interest in using porous ceramics as aerostatic bearing restrictors [1], due primarily to their higher flexural modulus.

In the course of developing a customised material for such restrictors, a range of porous alumina disc specimens has been produced using the capsule-free hot isostatic pressing method (HIP) developed by Ishizaki [2]. This HIPing technique does not require encapsulation of the component. Hence, the HIPing gas can penetrate the pore structure to prevent pore closure. This method for sintering has been reported to result in porous substrates of higher strength and more consistent pore structure than conventional pressureless sintering.

Both strength and elastic modulus are known to vary significantly with the level of porosity [3]. An understanding of strength-porosity and modulus-porosity relationships is of great importance to the air bearing designer who is interested in maximising strength and modulus for a required fluid flow through the bearing.

In this paper, flexural moduli and strength have been measured for a range of porous alumina specimens of different initial powder sizes and final porosities, sintered using the capsule-free hot isostatic pressing method. The dependence of these mechanical properties on total porosity has been investigated empirically.

2. Experimental procedure

2.1. Specimen preparation

Disc-shaped porous alumina specimens were produced from 100% α-alumina powders of mean particle size between 0.5 and 42 μm. Particle sizes of the powders were determined with a Micromeritics 5100 Sedigraph. Green bodies, of mean particle size greater than 7 μm, were consolidated by vibratory packing in boron-nitride coated, porous graphite tooling. For powder sizes of 7 μm or less, the vibration-packed green density was inadequate and hence discs were slip cast. Specimen size was 53 mm in diameter and 8 mm in height, in the green state [1].

The discs were subsequently hot isostatically pressed within graphite tooling using a capsule-free method. HIPing temperature ranged from 1600 °C to 1900 °C, with a 5-hour ramp, followed by an isothermal dwell of 1 to 2 hours, and subsequent furnace cooling. HIPing pressure varied between 500 and 1500 bar. This range of conditions produced specimens with total porosity, as a fraction of total volume, of between 0.1 and 0.44. An example of a porous alumina specimen, porosity 0.3, is shown in Fig. 1. Specimen density was measured using

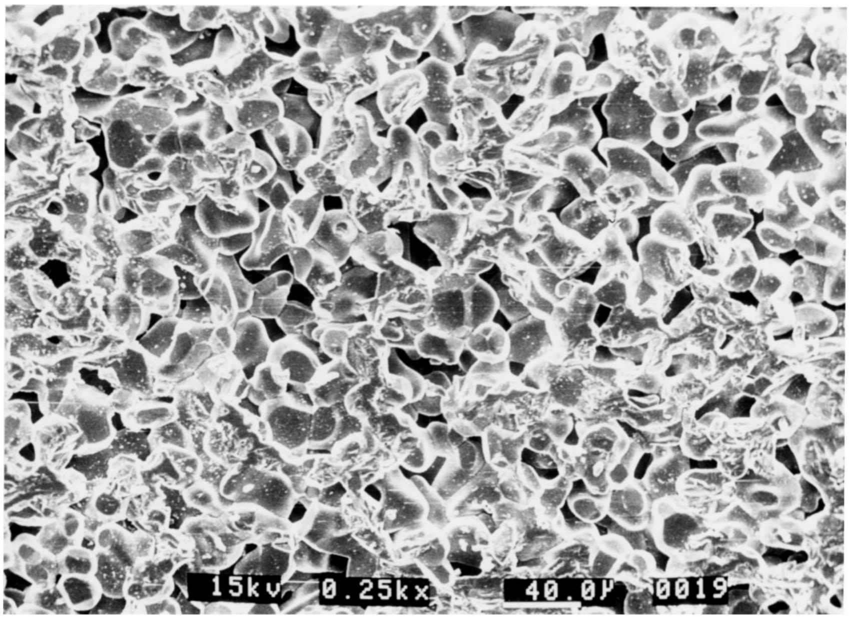

Figure 1 SEM micrograph of a HIPed porous alumina, porosity 0.3.

an adaptation of the ISO 2738 Archimedes method [1], using water as the impregnating medium.

The specimens were then diamond ground to 44 mm diameter to remove at least 0.5 mm from each specimen surface after sintering. Ultrasonic cleaning in ethanol and drying at 50 °C for 12 hours completed the specimen preparation process.

Disc specimens were also produced from a bi-modal mixture, where the mean particle size of the large-particle mode was between 42 and 400 μm, and the smaller particle mode was a 0.5 μm mean particle size powder. The weight percentage of the second mode was between 13 and 33%. For comparison, specimens sintered with a sintering aid (lithium fluoride) 1–4% by weight were also included. Machining and cleaning of the specimens were performed as described above.

2.2. Flexural modulus

The flexural modulus, shear modulus and the Poisson's ratio of the porous specimens were measured using the impulse excitation technique [4]. This was chosen in preference to the more widely used free-free beam resonance technique [5–7], as the latter would have required machining of all the disc specimens to a rectangular shape. A number of published reports [8, 9] have indicated that the impulse excitation technique produces results consistent with the standard methods for beam type specimens.

The impulse excitation method was carried out on a Lemmens GrindoSonic Mk5. Each disc specimen was supported on a piece of plastic foam material of very low stiffness. The specimen was then struck at selected nodal points with a 4 mm hardened steel ball, bonded to the end of a flexible plastic strip. The response was measured by a piezoelectric pick-up (Fig. 2). The elastic modulus, the shear modulus, and the Poisson's ratio were evaluated based on the dimensions and weight of the specimen [4].

2.3. Flexural strength

Fracture testing of disc-shaped specimens was carried out using the concentric ring loading method developed

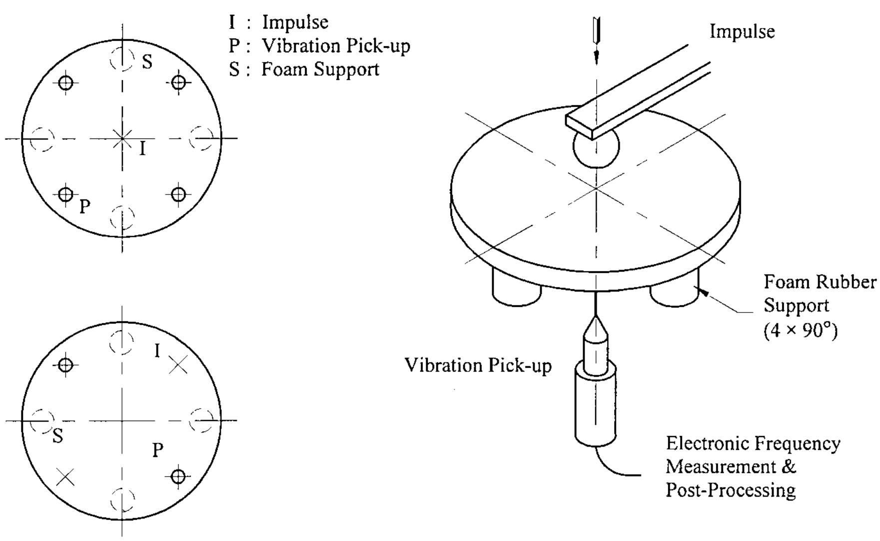

Figure 2 Schematic diagram of the impulse excitation technique for the measurement of flexural modulus.

by Godfrey [10], which has been successfully employed elsewhere [11, 12]. One particular advantage of this method is that the edges of the specimen are not subjected to load, and as such do not require a high quality surface finish.

Specimens were axially loaded to fracture in a compression testing machine (Instron 6025 with a 5 kN load cell of 0.5% accuracy) between two concentric rings of ball bearings. The outer supporting ring consisted of 69 bearing balls of 2 mm diameter on a 44 mm pitch circle seated on a hardened surface. The inner loading ring of 25 balls, also of 2 mm, had a pitch circle of 16 mm, and was held concentric to the former on the loading fixture. A ground conical centre, screwed onto the compression tester, engaged onto a centre hole on the top plate to ensure concentric loading and to minimise the effect of any angular misalignment between the compression tester and the specimen holder.

The bi-axial flexural failure stress was then calculated using the following equation:

$$\sigma_r = \sigma_t = \frac{3W_f}{2\pi \cdot z_p^2}\left[(1+\nu)\ln(r_s/r_l) + \frac{(1-\nu)\left(r_s^2 - r_l^2\right)}{2r_p^2}\right] \quad (1)$$

where σ_r is the stress in the radial direction; σ_t is the stress in the tangential direction; W_f is the load at failure for the fracture test; z_p is the thickness of the specimen; ν is the Poisson's ratio; r_s is the pitch radius of the ring fracture supporting balls; r_l is the pitch radius of the ring fracture loading balls; r_p is the radius of the specimen.

For comparison, disc specimens were sliced into small rectangular bars of approximately 40 mm × 6 mm × 4 mm, and fracture tested using a 4-point bend test. The point loading was applied through hardened needle rollers of 2 mm diameter, which were located in ground V-grooves to ±0.01 mm. The supporting rollers had a separation of 20 mm, the loading rollers 10 mm.

For the 4-point bend test, the flexural stress to failure is given by:

$$\sigma_f = \frac{3W_f b_l}{w_b z_b^2} \quad (2)$$

where σ_f is the flexural stress; W_f is the load at failure for the fracture test; b_l is the distance between a supporting and loading roller; w_b is the width of the specimen; z_b is the thickness of the specimen.

3. Results

3.1. Flexural modulus

The variation of flexural and shear moduli with total porosity is presented in Figs 3 and 4. Closed porosity was found to be negligible for all specimens. The two moduli appeared to have an approximately exponential relationship with porosity as total porosity approaches zero. As shown in Fig. 5, Poisson's ratio also increased, in an approximately linear fashion, with decreasing porosity.

The moduli data and Poisson's ratio were least-square fitted with three different functions:

i) Critical porosity (Phani) [13]

$$X = X_o(1 - \zeta/\zeta_{cr})^a \quad (3)$$

where X is the modulus or Poisson's ratio of the specimen; X_o is the modulus or Poisson's ratio at full density; ζ is the total porosity of the specimen; ζ_{cr} is known as

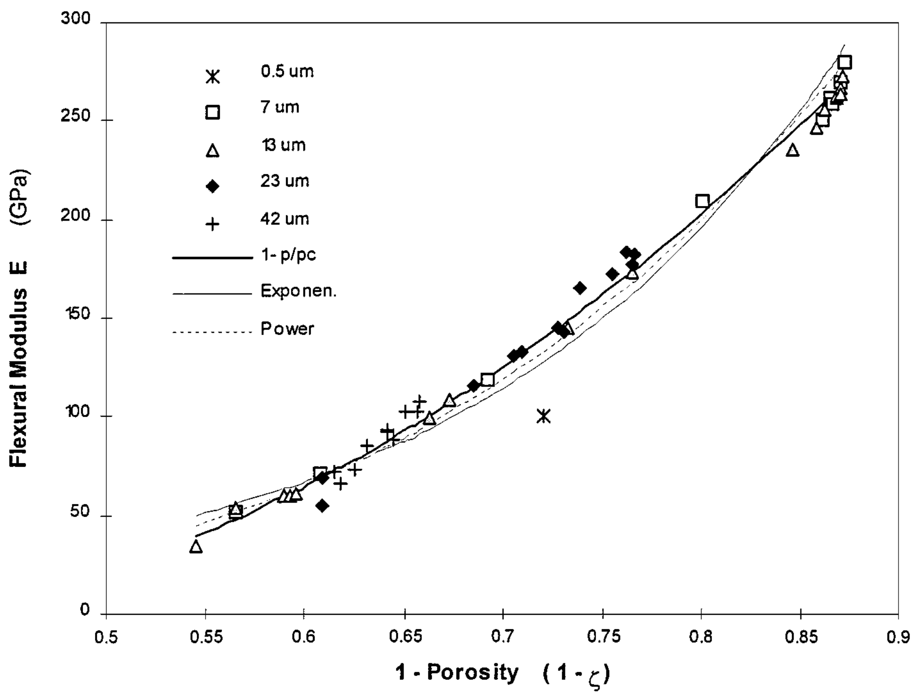

Figure 3 Graph of flexural modulus vs. porosity.

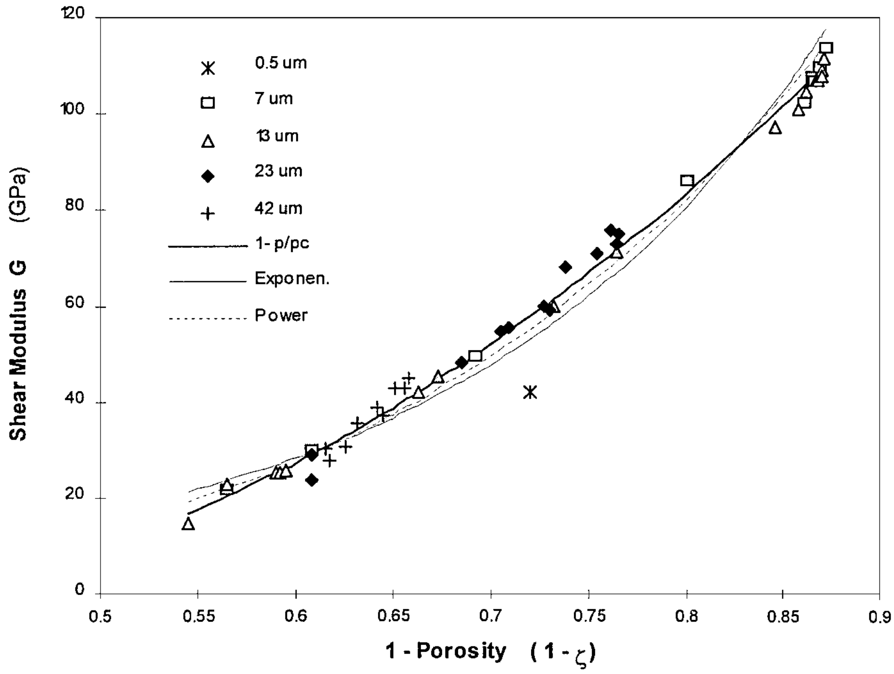

Figure 4 Graph of shear modulus vs. porosity.

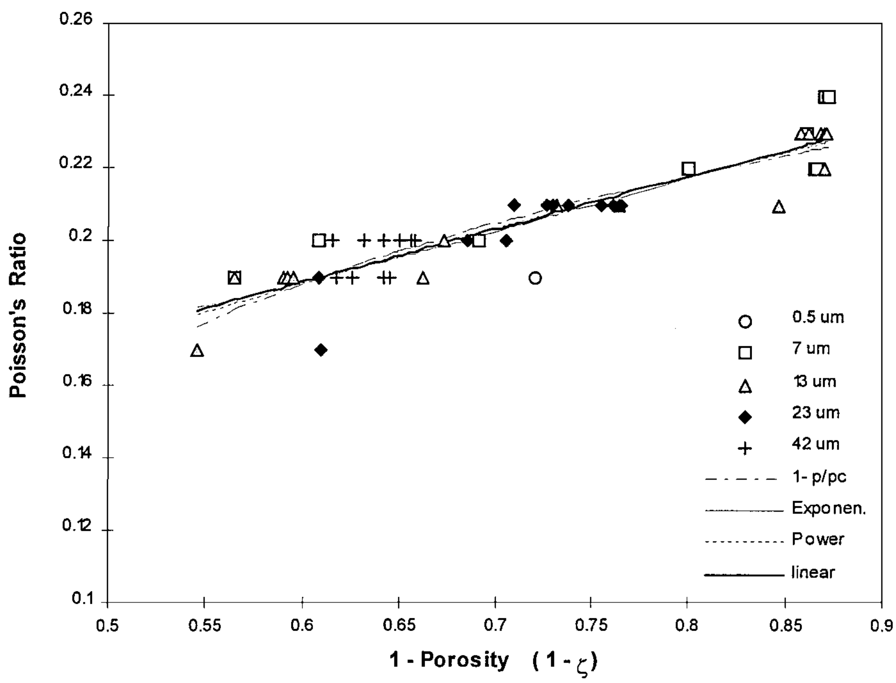

Figure 5 Graph of Poisson's ratio vs. porosity.

the critical porosity, at which the elastic modulus becomes zero [13].

The value of the critical porosity was determined numerically from the data by determining which critical porosity yielded the most accurate data fit.

ii) Power function (Wagh) [3]

$$X = X_0(1 - \zeta)^a \tag{4}$$

where a is a constant.

iii) Exponential function (Duckworth, Spriggs) [14, 15]

$$X = X_0 e^{-b\zeta} \tag{5}$$

where b is a constant.

The accuracies of the data fit of Equations 3 to 5, represented by the sum of the square of the relative error (R^2), are shown in Table I.

The extrapolated values of moduli and Poisson's ratio at zero porosity, and the empirically derived equation constants are summarised in Table II.

3.2. Flexural strength

The relationships between flexural strength and porosity are shown in Figs 6 and 7. Experimental results obtained in the course of the present work were divided into three categories—concentric-ring-fractured, 100% alumina disc specimens, 4-point-fractured, 100%

TABLE I Error of data fit of Equations 3 to 5, where R is the relative error

	$X = X_o (1 - \zeta/\zeta_{cr})^a$ [13] $\zeta_{cr} = 0.625$ ΣR^2	$X = X_o (1 - \zeta)^a$ [3] ΣR^2	$X = X_o e^{-b\zeta}$ [14] ΣR^2
Flex-modulus E (GPa)	0.25	0.36	0.56
Shear-modulus G (GPa)	0.24	0.34	0.54
Poisson's Ratio ν	0.053	0.057	0.051

TABLE II Empirically derived constants in the equations for elastic modulus, shear modulus and Poisson's ratio

	$X = X_o (1 - \zeta/\zeta_{cr})^a$ [13] $\zeta_{cr} = 0.625$		$X = X_o (1 - \zeta)^a$ [3]		$X = X_o e^{-b\zeta}$ [14]	
	X_o	a	X_o	a	X_o	b
Flex-modulus E (GPa)	409.5	1.82	479.7	3.91	576.1	5.38
Shear-modulus G (GPa)	165.4	1.78	193	3.82	230.8	5.26
Poisson's Ratio ν	0.239	0.234	0.244	0.508	0.25	0.71

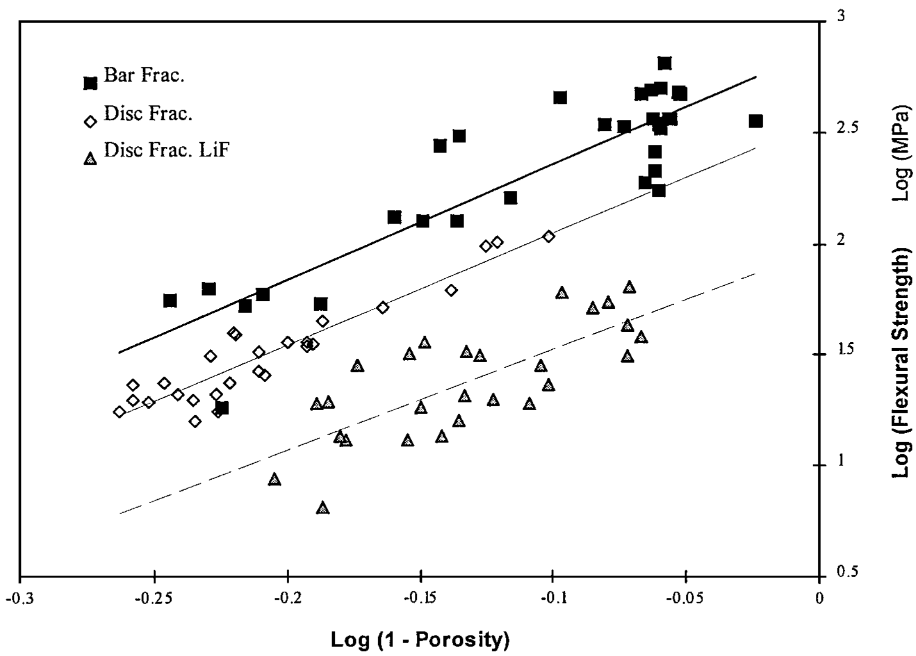

Figure 6 Graph of flexural strength vs. porosity (power law).

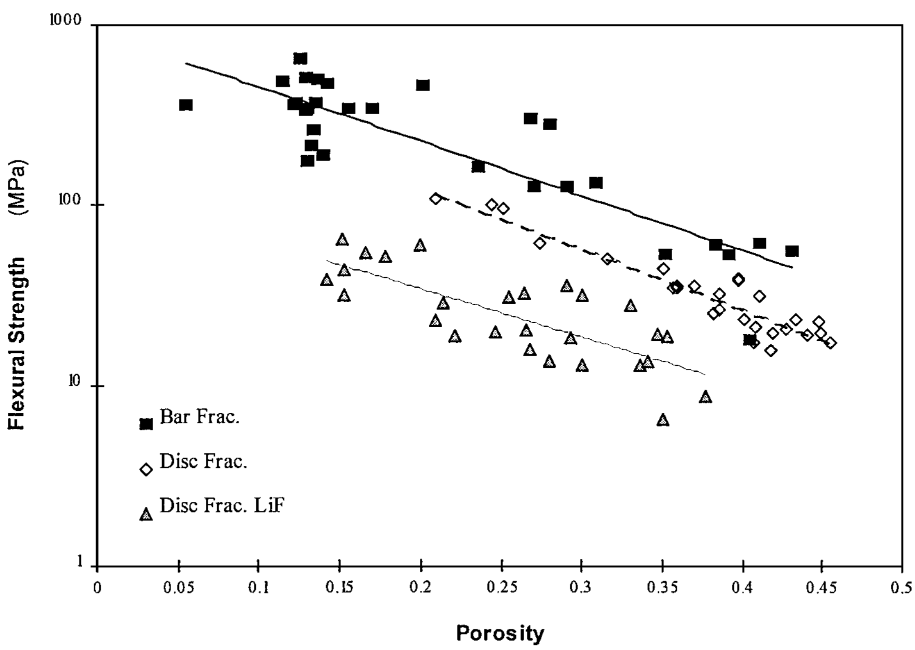

Figure 7 Graph of flexural strength vs. porosity (exponential).

TABLE III Empirically derived constants in the equations for flexural strength

	$\sigma = \sigma_o(1-\zeta)^c$ [16]		$\sigma = \sigma_o e^{-d\zeta}$ [14]	
Flexural strength (MPa)	σ_o	c	σ_o	d
Disc specimens	352	5.03	580	7.7
Bar specimens	745	5.16	893	6.9
Disc specimens with LiF	94.9	4.54	116	6.11

alumina bar specimens, and concentric-ring-fractured, disc specimens with sintering aid.

The data were least-square fitted to a power [16] and an exponential [14] function:

$$\sigma_f = \sigma_o(1-\zeta)^c \tag{6}$$

and

$$\sigma_f = \sigma_o e^{-d\zeta} \tag{7}$$

where σ_o is the theoretical flexural strength at full density and c and d are constants.

The relationship of strength to porosity follows a similar trend to that of the elastic moduli. The empirical constant c has a value approximately 5 for both bar and disc specimens, but a slightly lower value of 4.5 for specimens sintered with the sintering aid lithium fluoride. The flexural strength was highest for bar specimens, followed by disc specimens and those with lithium fluoride. The extrapolated strength at theoretical density, and the empirically derived equation constants are presented in Table III.

4. Discussion

4.1. Dependence of flexural modulus on porosity

The empirical relationship between flexural modulus and porosity of various materials has been extensively investigated, both theoretically and experimentally. Recent reviews have been published by Wagh [3] and Rice [17]. There are two main schools of thought. The first, represented by Duckworth [14] and Spriggs [15], attempted to describe the relationship with an exponential function (Equation 5). Others, amongst them Wagh [3], used a power law function (Equation 4) in which the constant a could be shown to be equal to b in the exponential function for low porosity values.

The power law model was first proposed by Phani and Niyogi [13] in a slightly different form (Equation 3), based on theory of elasticity of a continuum with the pores as a second phase. Wagh [3] argued that fitting of experimental data yielded $\zeta_{cr} = 1$, hence the simplified form in Equation 4.

No data for the Poisson's ratio dependence on porosity are known to the authors.

As shown in Table I, the empirical function based on the theory of Phani [13] appeared to provide a slightly better fit for the data. The critical porosity value ζ_{cr} of 0.625 was obtained numerically as the one that gave the least error of fit to measured data.

The flexural modulus E_o of fully-dense α-alumina is quoted as 410 GPa [18]. This can be compared against experimentally derived values of X_o for flexural modulus tabulated in Table II. Both of the mathematical models based on power laws appeared to give X_o values in better agreement with the accepted value.

Published values for the exponential a in Equation 2 [3] lie between 2 and 5. According to the theory proposed by Wagh, this value is an indirect measure of the 'tortuosity' of the pore network, with a higher value of a implying a wider distribution of pore cross-sectional area. Wagh obtained a value close to 2 for the constant, a, first theoretically and then experimentally for a large collection of specimens of various ceramics sintered under atmospheric pressure, but a value close to 4 for hot-pressed specimens and those with sintering aids. As shown in Table II, the fitted value obtained from the present work is 3.91, indicating a resemblance to hot pressing, suggesting a higher tortuosity. Table II also indicates that the constant, b, obtained from the exponential fit, which is expected to be equal to a in the simple power law model, has a slightly higher value.

The moduli data shown in Figs 3 and 4 are further subdivided into the mean particle size of the ceramic powder from which the specimens were sintered. No particle size related deviations from the general trends discussed above can be observed in the data. It should be mentioned, however, that the range of porosity for particle sizes above 23 μm were limited due to an upper limit on the HIPing temperature.

A comparison of Figs 3 and 4 show that the relationships of flexural and shear moduli to porosity are very similar. Again no particle-size based deviations in the relationship of shear moduli with porosity were observed.

4.2. Flexural strength dependence on porosity

The dependency of fracture properties on porosity has also been reported extensively. Wagh [16] extended his work on elastic constants to include flexural strength. Using the same power law model as in Equation 6, he conducted a theoretical analysis to deduce that the exponent, c, should be related to the constant, a, in Equation 4 by:

$$c = a + 0.5 \tag{9}$$

This was validated experimentally.

On the other hand, Duckworth [14] also used an exponential function (Equation 7) for the flexural strength, similar to his model for elastic constants.

With either model, the results from the current study (Table II) showed a consistently higher value of σ_o for the bar specimens, followed by that of disc specimens of 100% alumina, and then disc specimens with sintering aids. The lower values obtained in the concentric ring-fracture test can be attributed to the bi-directional stresses in an axi-symmetric loading system [10]. The use of sintering aids has been known to result in lower strength owing to the presence of weaker intergranular phases and this is confirmed by the experimental results. Again the Duckworth model consistently gives higher values of σ_o than that of Wagh.

The empirical constants c and d obtained here also differ from a and b (corresponding to the elastic constants) by more than 0.5, the value suggested by Wagh [16]. Such a discrepancy was also reported in Wagh's own work [16], although he attributed the discrepancy to a possible glassy phase in that particular set of specimens. As the constants are an indirect measure of the tortuosity, and the constants a and b have higher than expected values as deduced from elastic constants measurements, such deviation might also be attributed to the difference in pore structure between the specimens from the present work and those used by Wagh.

Similarly to the moduli data, no deviations in the relationship of strength with porosity owing to mean powder size effects were observed. This indicates that, as has been reported elsewhere [3], the Griffith flaw model of ceramic strength breaks down at high porosity, with strength becoming dependant on the cross-sectional area of solid material, rather than the 'weakest flaw.' Susceptibility of flexural strength to processing-route induced artefacts was also not observed. Specimens of powder size below 7 μm were slip cast, whilst those above this size were vibrationally packed, but there were no significant deviations from the overall porosity-strength relationship in either size range of specimen.

Contrary to reports by Ishizaki [19], no evidence could be drawn from the current results to indicate that the capsule-free HIPing method results in porous ceramics of higher strength than those sintered otherwise. Both the constants σ_o and c are of similar values to those reported elsewhere for alumina [18].

5. Conclusions

The elastic moduli and flexural strength for a range of capsule-free HIPed, porous alumina disc specimens of varying powder size and porosity have been measured, using the impulse excitation and the concentric-ring fracture methods respectively.

The dependency of these structural properties on the total porosity of the specimens has been investigated. Closed porosity was found to be negligible in the capsule-free HIPed specimens. The results indicated that both the power and the exponential functions could adequately describe the porosity dependency of flexural strength. The strength values obtained were test method dependent, with the 4-point bend test giving higher strength values. Strength values were, as expected, significantly lower for specimens with sintering aids. The theory by Phani (Equation 3), on the other hand, gave the best fit for the modulus data. No dependence on particle size was noticeable in either case.

It was not evident from the strength measurement data that better strength could be obtained by the capsule-free hot isostatic pressing method.

References

1. Y. B. P. KWAN, PhD thesis, Cranfield University, 1996.
2. K. ISHIZAKI and M. NANKO, *Journal of Porous Material* **1** (1995) 19.
3. A. S. WAGH, R. B. POEPPEL and J. P. SINGH, *Journal of Material Science* **26** (1991) 3862.
4. J. W. LEMMENS, "Dynamic Measurements in Materials," (American Society for Testing and Materials, Philadelphia, 1990).
5. W. R. DAVIS, *Transactions of the British Ceramics Society* **67** (1968) 515.
6. ASTM C 1198-91, ASTM Standards Vol. 15.01, (American Society for Testing and Materials, Philadelphia, 1991).
7. JIS R 1602-1986 (Japan Standards Association, Tokyo).
8. A. WOLFENDEN, K. HERITAGE and F. CLAYTON, *Review of Scientific Instruments* **59** (1988).
9. R. J. ALLISON and J. BOUTIN, *Deformation of Sediments and Sedimentary Rocks, Geological Society Special Publication* **29** (1987) 63.
10. D. J. GODFREY, *British Ceramic Proceedings* **39** (1987) 133.
11. S. M. FAVIER, MSc thesis, Cranfield Institute of Technology, 1990.
12. J. H. SHAW, S. M. BEST and W. BONFIELD, *Journal of Materials Science Letters* **14** (1995) 1055.
13. K. K. PHANI and S. K. NIYOGI, *ibid.* **6** (1987) 511.
14. W. DUCKWORTH, *Journal of American Ceramic Society* **36** (1953) 68.
15. R. M. SPRIGGS, *ibid.* **44** (1961) 628.
16. A. S. WAGH, POEPPEL and R. B. SINGH J. P., *Journal of Material Science*, **28** (1993) 3589.
17. R. W. RICE, *Materials Science and Engineering*, **A112** (1989) 215.
18. R. MORRELL, "Handbook of Properties of Technical and Engineering Ceramics," 1st ed. (HMSO, London, 1987).
19. A. TAKATA, K. ISHIZAKI, Y. KONDO and T. SHIOURA, *Materials Research Society Symposium Proceedings* **251** (1992) 133.

Received 26 January
and accepted 11 August 1999